

Singapore Management University

Institutional Knowledge at Singapore Management University

Research Collection School Of Computing and
Information Systems

School of Computing and Information Systems

6-2011

Online fault detection of induction motors using frequency domain independent components analysis

Zhaoxia WANG

Singapore Management University, zxwang@smu.edu.sg

C. S. CHANG

Follow this and additional works at: https://ink.library.smu.edu.sg/sis_research



Part of the [Numerical Analysis and Scientific Computing Commons](#), and the [Operations Research, Systems Engineering and Industrial Engineering Commons](#)

Citation

1

This Conference Proceeding Article is brought to you for free and open access by the School of Computing and Information Systems at Institutional Knowledge at Singapore Management University. It has been accepted for inclusion in Research Collection School Of Computing and Information Systems by an authorized administrator of Institutional Knowledge at Singapore Management University. For more information, please email cherylids@smu.edu.sg.

Online Fault Detection of Induction Motors Using Frequency Domain Independent Components Analysis

Z. Wang

Department of Computer Science,
Institute of High Performance Computing, Singapore 138623.
Email: wangz@ihpc.a-star.edu.sg

C.S. Chang

Department of Electrical and Computer Engineering,
National University of Singapore, Singapore 117576
Email: eleccs@nus.edu.sg

Abstract—This paper proposes an online fault detection method for induction motors using frequency-domain independent component analysis. Frequency-domain results, which are obtained by applying Fast Fourier Transform (FFT) to measured stator current time-domain waveforms, are analyzed with the aim of extracting frequency signatures of healthy and faulty motors with broken rotor-bar or bearing problem. Independent components analysis (ICA) is applied for such an aim to the FFT results. The obtained independent components as well as the FFT results are then used to obtain the combined fault signatures. The proposed method overcomes problems occurring in many existing FFT-based methods. Results using laboratory-collected data demonstrate the robustness of the proposed method, as well as its immunity against measurement noises and motor parameters.

Index Terms—Fast Fourier Transform (FFT), Fault detection, Features of the frequency signatures (FS features), Independent Component Analysis (ICA), Induction Motor.

I. INTRODUCTION

Early detection of electrical or mechanical anomalies in induction motors is very important for ensuring safe and economic operation of industrial processes [1]–[8].

Stator-current monitoring is viewed as an important fault-detection scheme without requiring special access to the motor [9]. Broken rotor-bars and bearing faults are two main fault types in induction motors [9]–[14], where most research was performed by decomposing and analyzing stator currents using various methods such as Fourier analysis, wavelets, neural networks, model-based techniques, and other statistical analysis [1]–[8], [11], [15]–[18].

Many of these methods are to find or monitor one or two frequency components which are related to the faults of the motor. These frequency analysis based methods are influenced by factors arising from noise and parameters of the motor, and are dependent on some necessary measurements [19]–[21].

In order to avoid the above drawbacks, this paper proposes a new fault detection method based on frequency-domain independent component analysis method. Unlike other frequency analysis based methods which have only one or two frequency components monitored, all the selected frequency components are used to calculate the features of the frequency signatures (FS features) in our proposed method. Thus, robust diagnosis

results can be obtained without considering or measuring the motor operating speed and other parameters of the motor.

Independent component analysis (ICA) is a special case of blind source separation, and has many practical applications such as signal processing [22] and biomedical engineering [23]. ICA can capture the essential structure of the data in many applications, including feature extraction and signal separation, because of its property of extracting statistically independent components.

We had proposed online fault detection methods of induction motors by analyzing the time-domain stator currents [5], [7]. The stator current data from motors are directly used to obtain independent components by employing ICA and to calculate time-domain features. Our successful attempt of using ICA on insulation diagnosis and online source recognition of partial discharge in gas insulated substations [24] and the stator current time-domain analysis induction motor fault detection [5]–[7] has established the foundation for this work.

This paper is divided into five sections. Section II presents the setup for collecting diagnostic data from laboratory induction motors. Section III provides the literature review of existing frequency-domain analysis methods and presents the challenges of these methods. Section IV presents our proposed frequency-domain independent component analysis method, which includes theoretical analysis, procedure of the proposed method, the formulation of the problem and solution, and performance compared to the existing frequency analysis based methods and our previous time-domain method. Section V concludes the paper.

II. EXPERIMENTAL SETUP

Fig. 1 shows our experimental setup for collecting stator-current waveforms from three identical motors of the same technical specifications but with different conditions: one being healthy, one having bearing fault and the other having broken rotor bars [5], [7]. The technical specifications are given in Table I.

The healthy motor is considered as a benchmark for comparing with the faulty conditions. Motor faults were artificially created with a dent on the seal, and the deformation of the

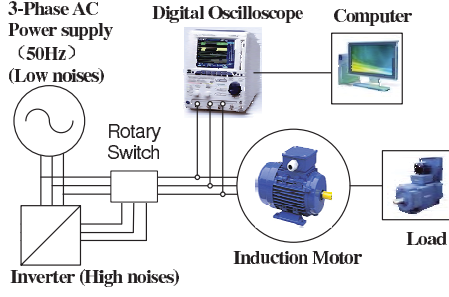


Fig. 1. Laboratory setup for data collection from induction motors

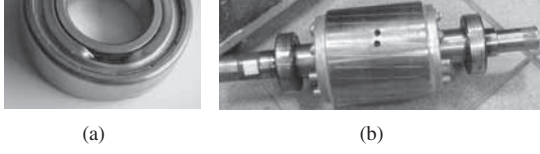


Fig. 2. Fault motors: (a) Denting the seal of the bearing to simulate bearing fault; (b) Two holes are drilled on the rotor bar to simulate broken rotor bar.

seal is connected to the inner race of the bearing as shown in Fig. 2(a), and two holes were drilled on the rotor bar of another motor as shown in Fig. 2(b).

Stator currents are measured separately with a 4-channel digital oscilloscope from each of the three motors. For collecting high noise signals, all induction motors are driven by the same voltage-fed pulse-width modulated inverter. 15 signal segments are collected from each motor at fixed frequency power supply without inverter (low noises) and with inverter (high noises). Fig. 3 illustrates the intercept parts of low noise signal (Fig. 3(a)) and the high noise signal (Fig. 3(b)).

III. FREQUENCY BASED ANALYSIS METHOD

A. Frequency-Domain Fault Signatures

FFT is the most widely used tool among the current frequency based analysis methods [1]–[9], [11]–[15]. FFT decomposes a time-domain signal into components of dif-

ferent frequencies. Motor stator current acts as an excellent transducer for detecting faults in motors. During operation, many harmonics will be present in a motor signal. FFT spectrum will thus show many peaks, including the fundamental frequency and its harmonics. This is known as the motor current signatures. Current signatures of faulty motors differ from those of healthy motors, because different electrical and mechanical faults generate different harmonics. Broken rotor-bar and bearing fault are two main fault types in induction motors [9]–[14].

A broken rotor-bar can be considered as a form of rotor asymmetry that causes unbalanced currents, decreased average torque and increased torque pulsations [9]–[11], [13], [14], [16], [18]–[20]. Monitoring the sidebands f_{br} around the fundamental harmonic is a widely used approach for diagnosing broken rotor-bars in induction motors in the following equation [9], [13], [14], [19], [20]:

$$f_{br} = f_s(1 \pm 2ks), k = 1, 2, 3, \dots \quad (1)$$

where

f_s electrical supply frequency;
 s per-unit slip.

Bearing faults take the form of outer-race, inner-race, ball or cage defects, which are the main causes of machine vibrations [9], [11], [19]–[21]. Vibrations due to bearing faults change the air-gap symmetry and machine inductances. Machine-inductance variations are reflected in the stator current in terms of current harmonics, which provide an indicator of bearing faults associated with mechanical oscillations in the air-gap. Bearing fault current harmonic frequencies f_{be} are expressed as [9], [20], [21]:

$$f_{be} = |f_s \pm m f_{i,v}| \quad (2)$$

where f_s is the fundamental supply frequency, $m = 1, 2, 3, \dots$ is the harmonic indexes and $f_{i,v}$ is one of the characteristic vibration frequency due to bearing faults.

$$f_{i,o} = \frac{n}{2} f_r \left[1 \pm \frac{bd}{pd} \cos \alpha \right] \quad (3)$$

where

n number of bearing balls;
 f_r mechanical rotor speed in Hz;
 bd ball diameter;
 pd bearing pitch diameter;
 α contact angle of the balls on the races.

Further explanation about the bearing faults can be found in [9], [20], [21]. Information about the bearing construction, which can be found in Table I, is required to calculate the exact characteristic frequencies as in Eqn. 3.

B. Challenges of Existing Frequency Based Analysis Method

As shown in Eqn. 1, the broken rotor-bar fault signatures (side-bands) depend on the slip. One significant challenge in the broken-rotor-bar detection is to distinguish its respective

TABLE I
PARAMETERS OF INDUCTION MOTORS FOR DATA COLLECTION

Motor Parameter		Bearing Parameter	
Power	1.1kW	Ball diameter, bd	8.89mm
Voltage (Δ/Y)	230/400V	Bearing pitch diameter pd	38.5mm
Current (Δ/Y)	4.5/2.6A	Number of bearing balls, n	12/13
Frequency	50Hz	Contact angle, α	0°
Speed	1410rpm	Bearing type:	NTN-6205Z
Pole pairs	2		

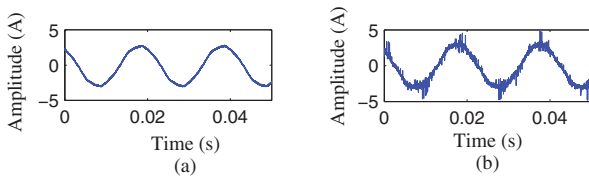


Fig. 3. Illustration of low noise waveform (a) and high noise waveform (b)

sidebands especially under low slip operation. Measured motor speed is required for calculating slip of the broken rotor-bar motors.

The physical parameters of the bearing are required in Eqns. 2 and 3 to calculate the bearing fault frequency. These can cause problems for detecting bearing faults if the bearing parameters are not known. Similar problems were also reported by other researchers [19].

IV. PROPOSED FREQUENCY INDEPENDENT COMPONENT ANALYSIS METHOD FOR ONLINE INDUCTION-MOTOR FAULT DETECTION

As mentioned in Section III, the fault-signature frequencies of broken rotor-bar and bearing fault are dependent of measurement or parameters of motors. If such information is not readily available, many frequency-domain techniques face problems in achieving reliable fault detection.

In order to overcome the above challenges, we propose a frequency-domain independent component analysis method. The proposed method does not require above operational dependent information. The necessary information required is stator current signals. The time-domain waveforms of the stator current signals are transferred to frequency-domain signals. All the frequency components, which include observed frequencies and unobserved frequencies (those are difficult to be observed, even though they exist according to Eqn. 1- 2), are used to calculate the features of frequency signatures of the signal. The proposed method overcomes the challenges mentioned in Section III.

A. Theoretical Analysis of the Proposed Method

The time-domain waveform of a stator current signal, $f(t)$, is presented by the following:

$$f(t) \rightarrow (f(t_1) \ f(t_2) \ \cdots \ f(t_L)) \quad (4)$$

where $f(t_i)$ ($i = 1, 2, \dots, L$) is amplitude at time t_i ($i = 1, 2, \dots, L$); L is a record length of samples. By using FFT, a frequency-domain signal $F(\omega)$ can be obtained from the time-domain waveform and can be represented by the following.

$$F(\omega) \rightarrow (a(\omega_1) \ a(\omega_2) \ \cdots \ a(\omega_N)) \quad (5)$$

where $a(\omega_i)$ ($i = 1, 2, \dots, N$) is the magnitude of frequency component ω_i ($i = 1, 2, \dots, N$). N is the selected number of the frequency components. We assume that Eqn. 5 represents a frequency-domain signal of the healthy motor. From the stator current signals of two faulty motors, $f_{br}(t)$ and $f_{be}(t)$, the frequency-domain signals of the faulty motors, $F_{br}(\omega)$ and $F_{be}(\omega)$ can be obtained and represented by the following:

$$F_{br}(\omega) \rightarrow (a_{br}(\omega_1) \ a_{br}(\omega_2) \ \cdots \ a_{br}(\omega_N)) \quad (6)$$

$$F_{be}(\omega) \rightarrow (a_{be}(\omega_1) \ a_{be}(\omega_2) \ \cdots \ a_{be}(\omega_N)) \quad (7)$$

where $a_{br}(\omega_i)$ ($i = 1, 2, \dots, N$) and $a_{be}(\omega_i)$ ($i = 1, 2, \dots, N$) are magnitudes of frequency components ω_i ($i = 1, 2, \dots, N$) of broken rotor bar motor and bearing fault motor, respectively.

The healthy motor is assumed to be ideal normal, and do not have any fault signatures. According to Eqns. 1 and 2,

the frequency-domain signal of the broken rotor bar motor has the sidebands around the fundamental harmonics, and the frequency-domain signal of the bearing fault motor is with the signatures of the bearing faults compared with that of the healthy motor. Therefore, Eqns. 5, 6 and 7 can be ideally represented by the following:

$$F_signals = \begin{pmatrix} a(\omega_1) \cdots a(\omega_n) & \overbrace{0 \cdots 0}^k & \overbrace{0 \cdots 0}^m \\ a(\omega_1) \cdots a(\omega_n) & a(\omega_{br1}) \cdots a(\omega_{brk}) & \overbrace{0 \cdots 0}^m \\ a(\omega_1) \cdots a(\omega_n) & \overbrace{0 \cdots 0}^k & a(\omega_{be1}) \cdots a(\omega_{bem}) \end{pmatrix} \quad (8)$$

Eqn. 8 can be simplified as:

$$F_signals = \begin{pmatrix} A_b & 0 & 0 \\ A_b & A_{br} & 0 \\ A_b & 0 & A_{be} \end{pmatrix} \quad (9)$$

where

$A_b = (a(\omega_1) \ a(\omega_2) \ \cdots \ a(\omega_n))$ represents the frequency characteristics of the healthy motor, which also are the basic characteristics of all the motors;

$A_{br} = (a(\omega_{br1}) \ a(\omega_{br2}) \ \cdots \ a(\omega_{brk}))$ represents the frequency characteristics of the motor with broken rotor bar;

$A_{be} = (a(\omega_{be1}) \ a(\omega_{be2}) \ \cdots \ a(\omega_{bem}))$ represents the frequency characteristics of bearing fault motor;

The first row of Eqn. 8 represents the magnitudes of different frequency components about the healthy motor as shown in the following:

$$F(\omega) \rightarrow \begin{pmatrix} A_b & \overbrace{0 \cdots 0}^k & \overbrace{0 \cdots 0}^m \end{pmatrix} \quad (10)$$

Eqn. 10 represents the magnitudes of healthy motor frequency signatures. Because the healthy motor is ideal normal, the magnitudes of faulty frequency components are zero. Similarly, the second row of Eqn. 8 shows the magnitudes of frequency signatures of broken rotor bar motor, and the magnitudes of bearing fault frequency components are zero as shown in Eqn. 11.

$$F_{br}(\omega) \rightarrow \begin{pmatrix} A_b & a(\omega_{br1}) \cdots a(\omega_{brk}) & \overbrace{0 \cdots 0}^m \end{pmatrix} \quad (11)$$

The third row shows the magnitudes of frequency signatures of bearing fault motor, and the magnitudes of broken rotor bar fault frequency components are zero as shown in Eqn. 12.

$$F_{be}(\omega) \rightarrow \begin{pmatrix} A_b & \overbrace{0 \cdots 0}^k & a(\omega_{be1}) \cdots a(\omega_{bem}) \end{pmatrix} \quad (12)$$

According to Eqns. 10, 11 and 12, different faults make their frequency-domain signals have different frequency signatures, and produce a series of different frequency components, such as A_{br} and A_{be} . According to above theoretical analysis, this paper proposes a new frequency-domain independent component analysis method. The proposed method solves the

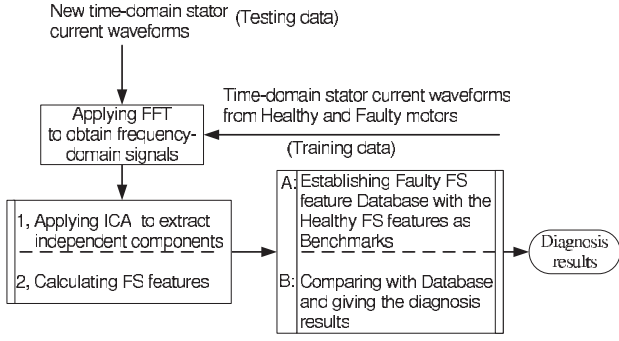


Fig. 4. The procedure of the proposed frequency-domain independent component analysis scheme

problems of the existing frequency analysis based methods. The robust results can be obtained regardless of the noises and other parameters or measurements of the motors. This makes the proposed method superior to our previous time-domain independent component analysis method.

B. Procedure of the proposed method

The procedure of the proposed frequency-domain independent component analysis scheme is shown in Fig. 4. The time-domain waveforms from healthy and faulty motors are converted into frequency-domain signals by using FFT in the first block.

In the second block, ICA algorithm is adopted to extract all the independent components from a chosen set of training data. After performing ICA on the chosen sets of training data, several obtained independent components are selected, and the FS features are calculated in the second block by using both frequency-domain signals and the selected independent components. To overcome the curse-of-dimensionality, it is always feasible to have low-dimensional data. For example, in this paper, two independent components are used to calculate the FS features. For other complex problems, more than two independent components can be used. As shown in Fig. 4, the second block has two step functions: 1st, extracting all the independent components and 2nd, calculating the FS features. The two step functions are employed for training data one by one. For testing data, only calculating the FS features is employed and the independent components used are obtained from training data.

The third block also has two functions: A and B. Function A is to establish Faulty FS feature Database with the healthy FS features as benchmarks by using the training data. Function B is to compare the FS features of test data with the established Database and giving the diagnosis results. The FS features of any new-time domain stator current waveforms can be obtained by using our proposed method, and compared with the Signature Database to arrive at the final fault diagnosis decision.

C. Formulation of the Proposed Frequency-Domain Independent Component Analysis

As shown in Fig. 4, time-domain stator current waveforms collected from healthy and faulty motors are transferred to the frequency-domain signals. ICA [5]–[7], [24], [25] is employed on the obtained frequency-domain signals for extracting the independent components by using the following:

$$IC = W \cdot F_Signals \quad (13)$$

As mentioned in the above section, the features of the frequency signatures (FS features) are calculated by using the extracted IC as well as the frequency-domain signals by using the following:

$$FS = F_Signals \bullet IC^T \quad (14)$$

Healthy and faulty frequency components in the frequency signatures shown in Eqns. 10, 11 and 12 all contribute to the FS features as shown in Eqn. 14. For example, any frequency domain signal $F(\omega)$ is converted to a M -dimension feature (from FS feature 1 to FS feature M) by using the independent components IC :

$$\begin{pmatrix} FS_1 & FS_2 & \dots & FS_M \end{pmatrix} = \begin{pmatrix} a(\omega_1) & \dots & a(\omega_N) \end{pmatrix} \times \begin{pmatrix} ic_{11} & \dots & ic_{1M} \\ ic_{21} & \dots & ic_{2M} \\ \dots & \dots & \dots \\ ic_{N1} & \dots & ic_{NM} \end{pmatrix} \quad (15)$$

where FS_1, FS_2, \dots, FS_M , represent FS feature 1, FS feature 2, ..., and FS feature M respectively. $F(\omega) = \begin{pmatrix} a(\omega_1) & \dots & a(\omega_N) \end{pmatrix}$ is a frequency-domain signal. It is transferred to a low-dimension FS feature (F_1, F_2, \dots, F_M) . In this paper, three independent components are extracted, and two independent components are selected for this problem, $M = 3$. The length of the frequency-domain signal is $N = 20000$. That means a higher dimension signal is mapped into a low dimension feature since $M \ll N$.

As shown in Eqn. 15, all the frequency components of a signal are used to compute the M -dimension FS features of the signal. For training data, all the M -dimension FS features of the signals from the healthy and faulty motors are exploited for establishing healthy and faulty signature database as shown in Fig. 4. To provide a holistic view of the fault signature database, each FS feature, which is obtained by using Eqn. 14, is normalized using the healthy motor as a benchmark for comparing with faulty conditions. After establishing the healthy and faulty signature database, each new signal of stator currents can be classified by using our proposed method.

D. Performance of our proposed Method

The performance of the proposed method is demonstrated by comparing to the existing frequency analysis based methods and our previous time-domain method.

As shown in Table II, the fault frequency of the motor with broken rotor bar can be estimated by using the parameters

TABLE II
NECESSARY PARAMETERS NEEDED AND ESTIMATED FAULT FREQUENCY
OF THE MOTOR WITH BROKEN ROTOR BARS

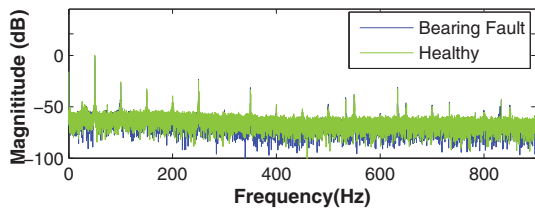
Fundamental frequency (Hz)	Measured/Estimated Rotor Speed (rpm)	Per-unit slip	Fault Signature Frequency f_b (Hz)
50	1461/1500	0.026	47.410/52.590

TABLE III
CALCULATED FAULT FREQUENCY OF THE MOTOR WITH BEARING FAULT
BY USING THE PARAMETERS IN TABLE I

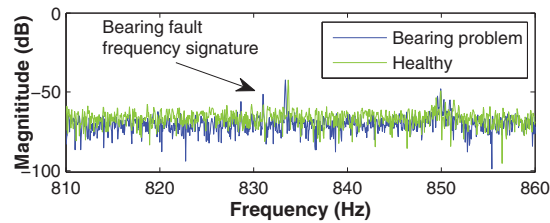
Fundamental frequency (Hz)	$f_{bearing}$ (Hz)
50	830.890

according to Eqn. 1. By using the parameters in Table I and Table III, fault frequency of the motor with bearing fault can be obtained as shown in Table III. The bearing fault frequency signatures compared with healthy frequency signatures using the existing frequency analysis methods are shown in Fig 5(a) and 5(b). Fig. 5(a) shows that it is difficult to locate bearing fault frequency without knowing the parameters of the motor. By using the parameters of the motor, we can locate the bearing fault frequency according to the Eqn. 2 and 3 as shown in Fig. 5(b). However, without using the parameters or measurement of the slip of the motors, our proposed method can give perfect classification results as shown in Fig. 6(a) and 6(b) under fixed frequency power supply without inverter (low noises) and with inverter (high noises). Fig. 6(c) and 6(d) show the results of our previous time-domain method under high noise condition.

Before de-noising the time-domain signals, the features



(a) Frequency-domain signal



(b) Locate bearing fault frequency by using the parameters of the motor

Fig. 5. Bearing fault frequency signatures by using existing frequency analysis method. (a) Difficult to locate bearing fault frequency without knowing the parameters; (b) Locating bearing fault frequency using the parameters of the motor

of the healthy and that of the bearing problems overlap each other. It is difficult to separate the signatures of the healthy motor from that of the bearing motor. The perfect results obtained by using our proposed method shows that the proposed method is independent of noises. This makes it superior to the time-domain ICA method. Moreover, Fig. 6(a) and Fig. 6(b) show that the two FS features have the same discriminative power, which implies that only one FS feature will be adequate via the use of a level detector for capturing the fault FS features of the three motors in this problems. According to Sections I and III, many presently available motor fault-detection techniques require the user some level of expertise about fault, operation and design-dependent information; which collectively make them difficult for online applications.

Using the scheme proposed in this paper, one however requires only a new signal of stator currents after establishing the Fault Signature Database. The subsequent online fault detection will be fully automatic. The proposed scheme is thus an ideal candidate for online monitoring of induction motors at remote locations, where manual inspections are expensive or even unavailable. Unlike our previous time-domain ICA [5] and hybrid time-frequency domain analysis method [7], a fuzzy neural network (FNN) or a fuzzy system are not required for the presently proposed scheme. The online fault detection would be 100% accurate judging from the superior performance of the classification as shown in Figs. 6(a) and 6(b).

V. CONCLUSION

A new scheme for online fault detection of induction motors is presented, which utilizes FFT to obtain frequency-domain signals, and then ICA to extract the independent components of the frequency signatures of stator-current signals. The extracted independent components as well as the frequency signals are then used to obtain features of the stator current. The proposed method overcomes challenges faced by many existing frequency analysis methods. It is demonstrated that our proposed frequency-domain independent component analysis provides robust, flexible, reliable and easy-to-implement fault detection on induction motors irrespective of measurement noises and motor parameters.

REFERENCES

- [1] K. Bimal, "Power Electronics and Motor Drives Recent Progress and Perspective," *IEEE Transactions on Industrial Electronics*, vol. 56, no. 2, pp. 581–588, 2009.
- [2] M. Khan and M. Rahman, "Development and implementation of a novel fault diagnostic and protection technique for IPM motor drives," *IEEE Transactions on Industrial Electronics*, vol. 56, no. 1, pp. 85–92, 2009.
- [3] F. Zidani, D. Diallo, M. El Hachemi Benbouzid, and R. Nait-Said, "A fuzzy-based approach for the diagnosis of fault modes in a voltage-fed PWM inverter induction motor drive," *IEEE Transactions on Industrial Electronics*, vol. 55, no. 2, pp. 586–593, 2008.
- [4] O. Alejandro, R. de Jesus, V. Alberto, R. Rooney, and G. Arturo, "Automatic online diagnosis algorithm for broken-bar detection on induction motors based on discrete wavelet transform for FPGA implementation," *IEEE Transactions on Industrial Electronics*, vol. 55, no. 5, pp. 2193–2202, 2008.

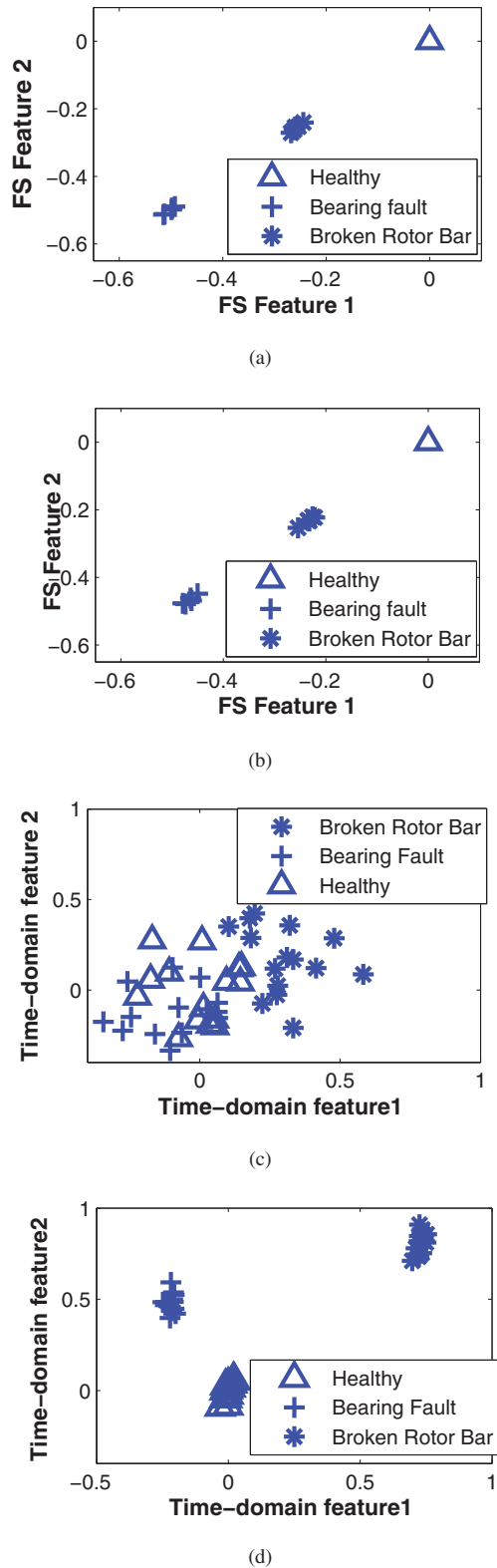


Fig. 6. Performance of the proposed method and comparison with time-domain method. (a) FS features obtained using low noise signals; (b) FS features obtained using high noise signals; (c) Time-domain results before de-noising by using our previous Ensemble and Individual Noise Reduction (EINR) Method [6]; (d) Time-domain results after de-noising by EINR Method.

- [5] Z. Wang, C. S. Chang, X. German, and W. W. Tan, "Online Fault Detection of Induction Motors Using Independent Component Analysis and Fuzzy Neural Network," in *8th IET International Conference on Advances in Power System Control, Operation and Management*, Hong Kong, 2009.
- [6] Z. Wang, C. S. Chang, T. Chua, and W. W. Tan, "Ensemble and Individual Noise Reduction Method for Induction-motor Signature Analysis," in *8th IET International Conference on Advances in Power System Control, Operation and Management*, Hong Kong, 2009.
- [7] T. Chua, W. W. Tan, Z. Wang, and C. S. Chang, "Hybrid Time-Frequency Domain Analysis for Inverter-Fed Induction Motor Fault Detection," in *IEEE International Symposium on Industrial Electronics, ISIE*, 2010.
- [8] S. Nandi, R. Bharadwaj, and H. Toliyat, "Performance analysis of a three-phase induction motor under mixed eccentricity condition," *IEEE Transaction on Energy Conversion*, vol. 17, no. 3, pp. 392–399, 2002.
- [9] M. Benbouzid, "Review of induction motors signature analysis as a medium for faults detection," *IEEE Transactions on Industrial Electronics*, vol. 47, no. 5, pp. 984–993, 2000.
- [10] G. Kliman, R. Koegl, J. Stein, R. Endicott, and M. Madden, "Noninvasive detection of broken rotor bars in operating inductionmotors," *IEEE Transaction on Energy Conversion*, vol. 3, no. 4, pp. 873–879, 1988.
- [11] B. Yazici and G. Kliman, "An adaptive statistical time-frequency method for detection of broken bars and bearing faults in motors using stator current," *IEEE Transactions on Industry Applications*, vol. 35, no. 2, pp. 442–452, 1999.
- [12] W. Thomson and M. Fenger, "Current signature analysis to detect induction motor faults," *IEEE Industry Applications Magazine*, vol. 7, no. 4, pp. 26–34, 2001.
- [13] A. Bellini, F. Filippetti, G. Franceschini, C. Tassoni, and G. Kliman, "Quantitative evaluation of induction motor broken bars by means of electrical signature analysis," *IEEE Transactions on Industry Applications*, vol. 37, no. 5, pp. 1248–1255, 2001.
- [14] C. Cunha, R. Lyra, and B. Filho, "Simulation and analysis of induction machines with rotor asymmetries," *IEEE Transactions on Industry Applications*, vol. 41, no. 1, pp. 18–24, 2005.
- [15] R. Schoen and T. Habetler, "Evaluation and implementation of a system to eliminate arbitraryload effects in current-based monitoring of induction machines," *IEEE Transactions on Industry Applications*, vol. 33, no. 6, pp. 1571–1577, 1997.
- [16] B. Ayhan, M. Chow, and M. Song, "Multiple signature processing-based fault detection schemes for broken rotor bar in induction motors," *IEEE Transactions on Energy Conversion*, vol. 20, no. 2, p. 336, 2005.
- [17] H. Su and K. Chong, "Induction machine condition monitoring using neural network modeling," *IEEE Transactions on Industrial Electronics*, vol. 54, no. 1, pp. 241–249, 2007.
- [18] B. Ayhan, M. Chow, and M. Song, "Multiple discriminant analysis and neural-network-based monolith and partition fault-detection schemes for broken rotor bar in induction motors," *IEEE Transactions on Industrial Electronics*, vol. 53, no. 4, p. 1298, 2006.
- [19] B. Akin, U. Orguner, H. Toliyat, and M. Rayner, "Low order PWM inverter harmonics contributions to the inverter-fed induction machine fault diagnosis," *IEEE Transactions on Industrial Electronics*, vol. 55, no. 2, pp. 610–619, 2008.
- [20] M. Benbouzid and G. Kliman, "What stator current processing-based technique to use for induction motor rotor faults diagnosis?" *IEEE Transaction on Energy Conversion*, vol. 18, no. 2, pp. 238–244, 2003.
- [21] J. Jung, J. Lee, and B. Kwon, "Online diagnosis of induction motors using MCSA," *IEEE Transactions on Industrial Electronics*, vol. 53, no. 6, pp. 1842–1852, 2006.
- [22] A. A. Amanatiadis and I. Andreadis, "Digital image stabilization by independent component analysis," *IEEE Transactions on Instrumentation and Measurement*, vol. 59, no. 7, pp. 1755 – 1763, 2010.
- [23] M. Crespo-Garcia, M. Atienza, and J. Cantero, "Muscle artifact removal from human sleep EEG by using independent component analysis," *Annals of Biomedical Engineering*, vol. 36, no. 3, pp. 467–475, 2008.
- [24] C. S. Chang, J. Jin, C. Chang, T. Hoshino, M. Hanai, and N. Kobayashi, "Online source recognition of partial discharge for gas insulated substations using independent component analysis," *IEEE Transactions on Dielectrics and Electrical Insulation*, vol. 13, no. 4, p. 892, 2006.
- [25] D. Tsai and S. Lai, "Independent component analysis-based background subtraction for indoor surveillance," *IEEE Transactions on Image Processing*, vol. 18, no. 1, pp. 158–167, 2009.